QLC-Based Design of Reference Tracking Controllers for Systems with Asymmetric Saturating Actuators

P. T. Kabamba, S. M. Meerkov, and H. R. Ossareh

Abstract— **Quasilinear Control (QLC) is a set of methods for designing reference tracking and disturbance rejection controllers for systems with nonlinear actuators and sensors. While most QLC methods are applicable to systems with symmetric nonlinearities, the current paper provides a technique for asymmetric ones, specifically, asymmetric saturating actuators. As in the symmetric case, the approach is based on the method of stochastic linearization, which reduces nonlinear systems to quasilinear ones. In the symmetric case, each nonlinear element is replaced by a gain. In the asymmetric case, however, each nonlinear element is replaced not only by a gain, but also by a bias. The latter leads to steady state errors incompatible with the usual error coefficients. Therefore, the performance of these quasilinear systems must be characterized not only by a root locus, but by another locus as well – the tracking error locus. In this paper these performance loci are characterized, methods for their calculation and sketching are presented, and the results are utilized for designing tracking controllers for random and deterministic reference signals.**

I. Introduction

Quasilinear Control (QLC) is a set of methods for designing linear controllers for systems with linear (or linearized) plants and nonlinear actuators and sensors. We refer to such systems as linear plant/nonlinear instrumentation (LPNI) systems. The main results of QLC are summarized in [1]. The approach is based on the method of stochastic linearization (SL), which reduces LPNI systems to quasilinear ones, with actuators and sensors represented by their equivalent gains. Unlike the usual, Jacobian linearization, SL is global; the price to pay is that the equivalent gains depend not only on the operating point but on all functional blocks and exogenous signals of the system. SL was first introduced in [2], [3]. A modern introduction to SL can be found in [4] and its pioneering applications to feedback control in [5], [6]. Conceptually, SL is akin the method of describing functions [7], but intended for transient and steady state analyses of nonlinear systems, rather than investigation of periodic solutions.

In [1], QLC theory has been developed for systems, where nonlinearities in actuators and sensors are odd functions and all exogenous signals have zero mean; roughly speaking, we refer to such systems as S-LPNI, where "S" stands for symmetric (see Section II for a precise definition). In practice, however, LPNI systems often have asymmetric nonlinearities, or non-zero mean reference signals, or both; we refer to such systems as A-LPNI, where "A" stands for asymmetric. Examples of these systems abound: air-conditioning/heating systems, flow control, automotive torque and idle speed control, wind turbine control, etc. Each of these systems has a saturating actuator and, for most operating points, this saturation is asymmetric. Therefore, extension of QLC to A-LPNI systems is of practical importance; clearly it is of theoretical importance as well.

Such an extension is not a trivial problem. The reason is that SL of asymmetric functions results in not only an equivalent gain but also an equivalent bias. In feedback environment, this bias leads to steady state errors incompatible with the usual error coefficients and may result in considerable loss of steady state performance. Investigation of quasilinear systems with equivalent gains and equivalent biases is the central problem of QLC for A-LPNI systems.

In the current paper such an investigation is carried out for A-LPNI systems with saturating actuators in the framework of the reference tracking problem. Along with the derivation of quasilinear gain and bias equations for such systems, we develop a method for tracking controllers design based on the so-called *performance loci*. These loci include the root locus for asymmetric saturating systems (*AS-root locus*) and tracking error locus (*TE locus*). Together, these loci are used for designing controllers that place closed loop poles and steady state tracking errors of quasilinear systems in appropriate admissible domains (defined by design specifications). Using this approach, the paper provides methods for designing controllers that track random and deterministic (e.g., step) signals. While the resulting controllers ensure the desired dynamic and steady state performance of quasilinear systems, stability properties of A-LPNI systems with these controllers can be ascertained using the usual methods of absolute stability [7]–[9], semi-global stability [10], [11], LMI-based approaches [12]–[14], etc.

Thus, the main contributions of this paper are:

- Introduction and development of performance loci for A-LPNI systems consisting of AS-root locus and TE locus.
- Methods for utilizing these loci for random and deterministic reference tracking controllers design.

Note that reference tracking controllers for systems considered in this paper can be designed using model predictive control [15]–[18] and anti-windup control [19]–[22]. Compared with the former, QLC is less computationally intensive – it does not require on-line solution of optimization problems. Compared with the latter, QLC provides a method for linear controller design in systems with saturating actuators, while anti-windup does not address the issue of controller

P. T. Kabamba is with the Aerospace Department, University of Michigan, Ann Arbor, MI, 48109, USA. email: kabamba@umich.edu. S. M. Meerkov and H. R. Ossareh are with the EE:Systems Department, University of Michigan, Ann Arbor, MI, 48109, USA. email: smm, hamido@umich.edu.

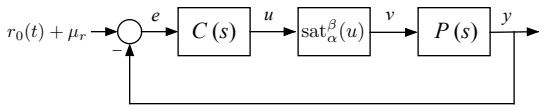

Fig. 1. LPNI system with saturating actuator.

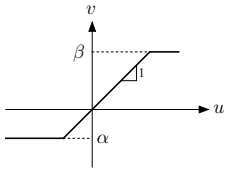

Fig. 2. Saturation function $\text{sat}_\alpha^\beta(u)$.

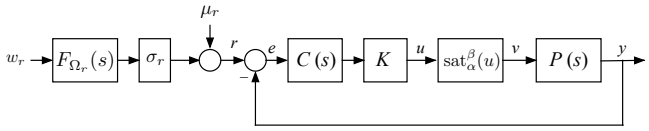

(a) LPNI system.

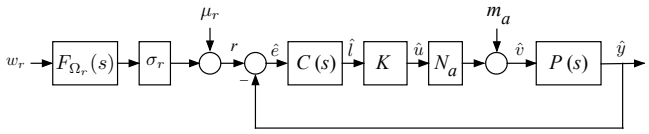

(b) Stochastically linearized system.

Fig. 3. LPNI system and its stochastic linearization.

design, but offers a mechanism to limit controller windup due to a pole at the origin.

The outline of this paper is as follows: Section II introduces a formal definition of symmetric and asymmetric LPNI systems. In Section III, equations for equivalent gain and bias in A-LPNI systems are discussed. AS-root locus and TE locus are introduced and developed in Section IV. Using these loci, Sections V and VI present methods for tracking controllers design of random and deterministic reference signals, respectively. Conclusions and topics for future work are given in Section VII. All proofs are included in the Appendix.

II. Definition of S- and A-LPNI Systems

Consider the SISO LPNI system shown in Fig. 1, where $P(s)$ and $C(s)$ are the plant and the controller, $r_0(t)$ is a zero-mean finite-power signal, μ_r is a constant, e, u, v, and y are the error signal, controller, actuator, and plant outputs, respectively, and $\text{sat}_\alpha^\beta(\cdot)$ is the saturation function (Fig. 2), with α and β being the lower and upper limits of saturation.

Definition 1. The LPNI system of Fig. 1 is *symmetric* (or S-LPNI) if

$$\frac{C_0}{1+C_0P_0}\mu_r = \frac{\alpha+\beta}{2}, \tag{1}$$

where P_0 and C_0 are the dc-gains of the plant and controller, respectively. Otherwise, it is *asymmetric* (or A-LPNI).

The reason for this definition is that under (1), the expected value of the signal u at the input of the saturation is at the center of its symmetry, i.e., $\mu_u = \frac{\alpha+\beta}{2}$. Thus, even if the saturation is symmetric ($\beta = -\alpha$), the system may or may not be symmetric depending on the dc-gains of the plant and controller and, most importantly, the average value of the reference signal (i.e., the set point, which may change during system operation).

As mentioned in the Introduction, symmetric systems with $\mu_r = 0$ and $\beta = -\alpha$ have been addressed in [1]. In the current paper, we consider the general case.

III. Stochastic Linearization of A-LPNI Systems with Saturating Actuators

This section reviews stochastic linearization of the LPNI systems considered in this paper. The details can be found in [23].

Consider the closed loop system of Fig. 3(a), where $P(s)$ is the plant, $KC(s)$ ($K > 0$) is the controller, $\text{sat}_\alpha^\beta(u)$ is the saturation function shown in Fig. 2, and $F_{\Omega_r}(s)$ is the third order Butterworth filter with bandwidth Ω_r and dc-gain selected to yield H_2 norm equal to 1, i.e.,

$$F_{\Omega_r}(s) = \sqrt{\frac{3}{\Omega}}\frac{\Omega^3}{s^3+2\Omega s^2+2\Omega^2 s+\Omega^3}. \tag{2}$$

We assume that the reference $r(t)$ is a random process obtained by filtering the Gaussian white noise $w_r(t)$ through $F_{\Omega_r}(s)$ and scaling and shifting the output by σ_r and μ_r, respectively. To define stochastic linearization of this system, introduce the following two functions:

$$\mathcal{F}_N(\sigma,\mu) = \frac{1}{2}\left[\text{erf}\left(\frac{\beta-\mu}{\sqrt{2}\sigma}\right) - \text{erf}\left(\frac{\alpha-\mu}{\sqrt{2}\sigma}\right)\right], \tag{3}$$

$$\begin{aligned}\mathcal{F}_M(\sigma,\mu) = {} & \frac{\alpha+\beta}{2} - \frac{\beta-\mu}{2}\text{erf}\left(\frac{\beta-\mu}{\sqrt{2}\sigma}\right) \\ & + \frac{\alpha-\mu}{2}\text{erf}\left(\frac{\alpha-\mu}{\sqrt{2}\sigma}\right) - \frac{\sigma}{\sqrt{2\pi}}\times \\ & \left[\exp\left(-(\frac{\beta-\mu}{\sqrt{2}\sigma})^2\right) - \exp\left(-(\frac{\alpha-\mu}{\sqrt{2}\sigma})^2\right)\right],\end{aligned} \tag{4}$$

where σ and μ are running variables, and $\text{erf}(x) = \frac{2}{\sqrt{\pi}}\int_0^x e^{-t^2}dt$ is the error function. Then, as derived in [23], the stochastically linearized version of this system is shown in Fig. 3(b), where

$$m_a = \frac{\mu_r}{P_0} - (\frac{1}{KC_0P_0} + N_a)\mu_{\hat{u}}, \tag{5}$$

and N_a and $\mu_{\hat{u}}$ are the solutions of the two transcendental equations

$$N_a - \mathcal{F}_N\left(K\left\|\frac{F_{\Omega_r}(s)C(s)}{1+P(s)KN_aC(s)}\right\|_2\sigma_r, \mu_{\hat{u}}\right) = 0, \tag{6}$$

$$\frac{\mu_r}{P_0} - \frac{\mu_{\hat{u}}}{KC_0P_0} - \mathcal{F}_M\left(K\left\|\frac{F_{\Omega_r}(s)C(s)}{1+P(s)KN_aC(s)}\right\|_2\sigma_r, \mu_{\hat{u}}\right) = 0, \tag{7}$$

with $\mathcal{F}_N$ and $\mathcal{F}_M$ given in (3) and (4). Here, $\|\cdot\|_2$ denotes the H_2 norm, $\mu_{\hat{u}}$ is the expected value of signal $\hat{u}$ in Fig. 3(b), and $K\|\frac{F_{\Omega_r}C}{1+PKN_aC}\|_2\sigma_r$ is the standard deviation of $\hat{u}$. It is shown in [23] that $0 < N_a < 1$. The gain N_a and bias

m_a in Fig. 3(b) are referred to as quasilinear (or equivalent) gain and bias, respectively.

A sufficient condition for existence of a solution of (6), (7), derived in [23], is:

(a) $1+\gamma P(s)C(s)$ has all zeros in the open left half plane for all $\gamma \in (0,1)$.
(b) If $C_0=\infty$ or $P_0=\infty$, then $\alpha < \frac{\mu_r}{P_0} < \beta$.

Solutions of (6), (7) may be found using a plethora of numerical techniques, e.g., the 2-variable bisection algorithm. In the Matlab computational environment, the "fsolve" function provides a convenient method for solving these equations.

It is shown in [23] that, if the plant is sufficiently slow as compared with the bandwidth of the input reference, stochastic linearization provides an accurate approximation of the original LPNI system as far as prediction of the mean and standard deviation of the output y is concerned. Therefore, the stochastically linearized system can be used for the purpose of controller design.

IV. Performance Loci for A-LPNI Systems

As one can see from Figure 3(b), the quasilinear gain, N_a, and the quasilinear bias, m_a, enter the system as an additional gain and input disturbance, respectively. Also, as can be seen from (6) and (7), both of them are functions of the controller gain, K. Thus, to characterize the system behavior as K changes from 0 to ∞, the behavior of quasilinear poles and quasilinear steady state errors as a function of K must be investigated. As mentioned in the Introduction, this leads to two loci: the usual one – root locus, and a novel one – tracking error locus. Together, they are referred to as performance loci. In this section, these loci, referred to as AS-root locus and TE locus, respectively, are characterized and methods for their calculation and sketching are presented. In the subsequent sections these loci are used for tracking controllers design.

A. Preliminaries

To begin, we group together the controller gain K and quasilinear gain N_a in Fig. 3(b) and denote the product by the *effective gain* K_e:

$$K_e(K) = KN_a(K).$$

Clearly, using (6), (7), for each $K>0$, $K_e(K)$ and $\mu_{\hat{u}}$ can be obtained by solving

$$K_e - K\mathcal{F}_N(K\left\|\frac{F_{\Omega_r}(s)C(s)}{1+P(s)K_eC(s)}\right\|_2\sigma_r,\mu_{\hat{u}})=0, \tag{8}$$

$$\frac{\mu_r}{P_0}-\frac{\mu_{\hat{u}}}{KC_0P_0}-\mathcal{F}_M(K\left\|\frac{F_{\Omega_r}(s)C(s)}{1+P(s)K_eC(s)}\right\|_2\sigma_r,\mu_{\hat{u}})=0. \tag{9}$$

Throughout this paper, we assume that the solution of the above equations exists and is unique.

Denote by $\mu_{\hat{e}}$ the mean of the error signal $\hat{e}$ in the quasilinear system, which can be expressed as

$$\mu_{\hat{e}}(K)=\frac{\mu_{\hat{u}}(K)}{KC_0}. \tag{10}$$

Based on the above notations, we introduce the following definitions.

Definition 2. The saturated closed loop poles (AS-poles) of the system of Fig. 3(a) are the poles of the system of Fig. 3(b), i.e., the poles of the transfer function from r to $\hat{y}$:

$$T(s)=\frac{K_e(K)C(s)P(s)}{1+K_e(K)C(s)P(s)}. \tag{11}$$

Definition 3. The AS-root locus is the path traced by the AS-poles when K changes from 0 to ∞.

Definition 4. The TE locus is the plot of $|\mu_{\hat{e}}(K)|$ as K changes from 0 to ∞.

Below, we develop the AS-root locus and the TE locus and investigate their properties.

B. The AS-root locus

In equation (11), $K_e(K)$ enters the transfer function as a usual gain. Furthermore, since $0<N_a<1$, we have that $0\le K_e(K)<K$. Therefore, the AS-root locus is a proper subset of the usual linear root locus. As in the linear root locus, we are interested in the points of origin and termination of the AS-root locus. Clearly, since $K_e(K)=0$ when $K=0$, the points of origin of the AS-root locus are the same as the linear root locus (i.e., at the poles of $P(s)C(s)$). The termination points, however, may not necessarily be at the open loop zeros. This is because $K_e(K)$ may not tend to infinity as K tends to infinity. Therefore, we equip the AS-root locus with the so-called AS-termination points. In addition, saturation may lead to output truncation. To account for this phenomenon, we equip the AS-root locus with the so-called AS-truncation points, beyond which the output does not follow the reference. Below, methods for computing both AS-termination and AS-truncation points are provided.

1) Calculating AS-termination points: Denote by K_e^* the limiting effective gain, i.e.,

$$K_e^*=\lim_{K\to\infty}K_e(K).$$

Clearly, if $K_e^*=\infty$, the termination points are the open loop zeros and the AS-root locus coincides with the usual root locus. However, if $K_e^*<\infty$, the root locus terminates prematurely. As it turns out, to compute K_e^*, the following two equations in the unknowns ϕ^* and η^* must first be solved:

$$\phi^*-\left\|\frac{F_{\Omega_r}(s)C(s)}{1+\frac{\beta-\alpha}{\sqrt{2\pi}\phi^*}e^{-\frac{\eta^{*2}}{2}}P(s)C(s)}\right\|_2\sigma_r=0, \tag{12}$$

$$\frac{\mu_r}{P_0}-\frac{\phi^*\eta^*}{C_0P_0}=\frac{\alpha+\beta}{2}+\frac{\beta-\alpha}{2}\mathrm{erf}(\frac{\eta^*}{\sqrt{2}}). \tag{13}$$

Note that (12) always has a solution $\phi^*=0$. There may be positive solutions as well, which lead to the following theorem.

Theorem 1. *Assume that $K_e(K)$ and $\mu_{\hat{u}}(K)$ exist and unique for all K. Then,*

1) if $\phi^*=0$ is the only solution of (12), (13), *$K_e^*=\infty$.*

2) if there exists another solution, $\phi^* > 0$, then

$$K_e^* = \frac{\beta - \alpha}{\sqrt{2\pi}\phi^*} e^{-(\frac{\eta^{*2}}{2})}. \quad (14)$$

Proof. See Appendix. ■

Definition 5. If $K_e^* < \infty$, the AS-termination points are the poles of the transfer function

$$T_{ter}(s) = \frac{K_e^* C(s)P(s)}{1 + K_e^* C(s)P(s)}. \quad (15)$$

Equations (14) and (15) are used to calculate the AS-termination points, which are marked by white squares on the AS-root locus. In Section V, we use this locus to select the gain K of the controller, which satisfies the dynamic tracking quality specifications.

2) The AS-truncation points: The AS-truncation points are introduced based on the notion of Trackable Domain, TD, which is the set of all step functions that can be tracked at steady state, with the usual linear tracking error $\frac{1}{1+C_0P_0}\mu_r$. Trackable domain for the symmetric case has been quantified in [1]. It is possible to show that for the asymmetric case, TD is given by

$$TD = \Big\{ r_0 : \Big| \frac{1}{KC_0} + P_0 \Big| \alpha < r_0 < \Big| \frac{1}{KC_0} + P_0 \Big| \beta \Big\}.$$

In the subsequent discussion, we assume, for simplicity, that $C_0 > 0$, $P_0 > 0$, and $\mu_r \in TD$ for all $K > 0$. We now introduce the proper extension of the so-called quality indicator I_0 introduced in [1]. This indicator quantifies the degree of amplitude truncation. Based on TD, we define I_0 as:

$$I_0 = \max\{ \frac{\sigma_r}{(\frac{1}{KC_0} + P_0)\beta - \mu_r}, -\frac{\sigma_r}{(\frac{1}{KC_0} + P_0)\alpha - \mu_r} \}.$$

Clearly, I_0 depends on K. Therefore, we denote it by $I_0(K)$. As a rule of thumb, amplitude truncation is typically small when $I_0(K) < 0.4$ (see [1]). Based on this idea, the following definition for the S-truncation points is introduced.

Definition 6. The AS-truncation points are the poles of

$$T_{tr} = \frac{K_e(K_{I_0})C(s)P(s)}{1 + K_e(K_{I_0})P(s)C(s)},$$

where

$$K_{I_0} = \min_{K>0} \{ K : I_0(K) = 0.4 \}.$$

Since the termination points occur when K tends to infinity, the AS-truncation points, when they exist, must occur prior to the AS-termination points. We use black squares to denote the AS-truncation points on the AS-root locus.

Example 1. Consider the system of Fig. 3(a) with

$$C(s) = 1, P(s) = \frac{s + 20}{(s + 15)(s + 0.5)}, \sigma_r = 1,$$

and $F_{\Omega_r}(s)$ as the third order butterworth filter (2) with bandwidth $\Omega_r = 1$. Initially, assume that $\alpha = -0.92$, $\beta = 0.92$, and $\mu_r = 0$. This system, which, according to Definition 1, is symmetric for all K, has been studied in Example 5.3 of [1]. Specifically, it has been shown that $K_e^* = \infty$ (i.e., the termination points are at the open loop zeros). Now, assume that $\mu_r = 1$, i.e., the system is asymmetric. The limiting effective gain K_e^*, calculated using Theorem 1, becomes $K_e^* = 21.4$. The AS-termination points, therefore, are at $-18.5 \pm 9.8j$ instead of the open loop zeros. Furthermore, the gain K_{I_0} calculated using Definition 6 is 0.88, and the AS-truncation points are at -14.7 and -1.5. The complete AS-root locus is shown in Fig. 4, where, as before, the white squares denote AS-termination points, the black squares denote the AS-truncation points, the x's denote open loop poles and the circle denotes the open loop zero. The shaded area is referred to as the "admissible domain", which is discussed in Section V. Note that, in this example, the truncation points are close to the open loop poles, which, as we show in Section V, implies that amplitude truncation takes place even for small values of controller gain.

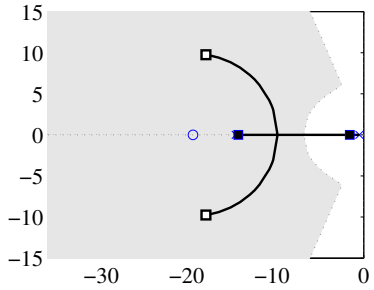

Fig. 4. AS-root locus.

C. TE locus

The TE locus may be plotted for each K using equations (8)-(10). As it turns out, it can be either increasing, or decreasing, or even non-monotonic function of K. As an example, consider the A-LPNI system of Fig. 3(a), with

$$C(s) = \frac{s + 0.1}{s + 1}, P(s) = \frac{1}{s + 1}, \alpha = -0.5, \beta = 1.5, \quad (16)$$

$\sigma_r = 1$, and F_{Ω_r} given by (2) with $\Omega_r = 1$. Fig. 5 shows the TE locus for three different μ_r's. Clearly, for $\mu_r = 0$, TE locus is increasing for all K, for $\mu_r = 0.5$ it is decreasing for all K, and for $\mu_r = -0.5$ it is non-monotonic. Furthermore, for $\mu_r = 0$ and $\mu_r = -0.5$, this locus does not tend to zero and as K tends to infinity. This is in contrast with linear systems, in which large K implies arbitrarily small steady state tracking error. Note that graph for $\mu_r = -0.5$ implies that the steady state tracking error may be as large as 70%.

The TE loci of Fig. 5 have been constructed by solving equations (8)-(10) for various K's. The following theorem provides a way for sketching TE locus without solving these equations, but using the properties of TE at $K = 0$ (origination), $K = \infty$ (termination), and an intermediate K for which the system is symmetric.

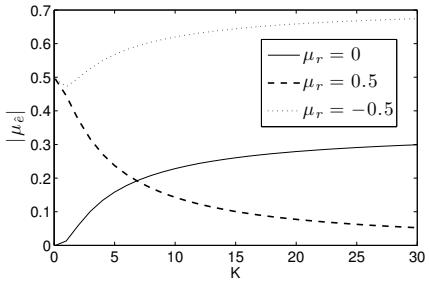

Fig. 5. TE locus for system (16) for different values of μ_r

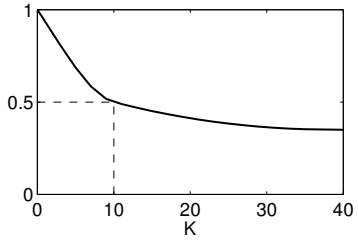

Fig. 6. The TE locus for system (16) with $\mu_r = 1$

Theorem 2. *Assume that* $\alpha \leq 0 \leq \beta$ *and that* (8), (9) *admit unique solutions for all* K. *Then,* $|\mu_{\hat{e}}(K)|$ *has the following properties:*

a. $\lim_{K\to 0^+} |\mu_{\hat{e}}(K)| = |\mu_r|$;
b. $\lim_{K\to 0^+} \frac{d|\mu_{\hat{e}}(K)|}{dK} < 0$;
c. $\lim_{K\to\infty} |\mu_{\hat{e}}(K)| = |\frac{\phi^*\eta^*}{C_0}|$, *where* ϕ^* *and* η^* *are the solution of* (12) *and* (13);
d. If $\frac{\mu_r}{P_0} > \frac{\alpha+\beta}{2}$, *then* $|\mu_{\hat{e}}(K)| = |\frac{\mu_r}{1+KP_0C_0}|$, *where* $K = \frac{1}{C_0(\frac{\mu_r}{\frac{\alpha+\beta}{2}} - P_0)}$

Proof. See Appendix. ■

For instance, applying this theorem to the above example (system (16)) with $\mu_r = 1$ we obtain:

$$|\mu_{\hat{e}}(0)| = 1, |\mu_{\hat{e}}(\infty)| = 0.35, |\mu_{\hat{e}}(10)| = 0.5. \qquad (17)$$

Therefore, the TE locus can be sketched as shown in Fig. 6.

Returning to Example 1, the TE locus of the system is plotted in Fig. 7. This locus originates at $|\mu_{\hat{e}}(0)| = 1$ and terminates at $|\mu_{\hat{e}}(\infty)| = 0.016$.

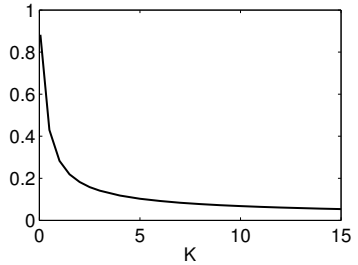

Fig. 7. The TE locus for Example 1.

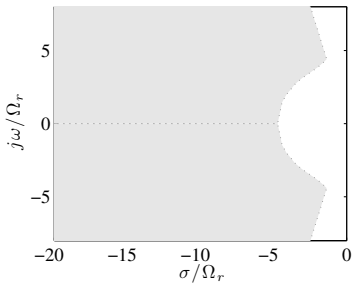

Fig. 8. Admissible domain.

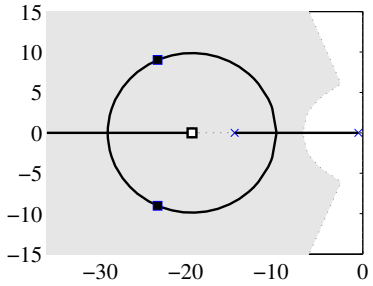

Fig. 9. AS-root locus with $\beta = 1.3$.

V. Design of Random Reference Tracking Controllers for A-LPNI Systems

A. Design for required dynamic performance

We first review the notion of admissible domain introduced in [1]. The admissible domain is the shaded area shown in Fig. 8 and is dependent on the bandwidth Ω_r of the coloring filter (see the axes in Fig. 8). If the AS-poles are within this domain, the dynamic quality of tracking is good.

The design goal is to choose gain K so that all AS-poles are within the admissible domain and positioned prior to the AS-truncation points. Note that there exists a fundamental trade-off in the size of K: it must be large enough to achieve static responsiveness, but small enough to avoid amplitude truncation.

Returning to the AS-root locus of the system in Example 1 (see Fig. 4), the AS-truncation points are outside the admissible domain; therefore, quality of tracking is bad due to amplitude truncation. To alleviate this problem, the authority of the actuator must be increased. With $\beta = 1.3$, the termination gain is $K_e^* = 10^4$ and the truncation gain K_{I_0} is 39. The AS-root locus for this case is shown in Fig. 9. Selecting $4 < K < 39$, the AS-poles are within the admissible domain and prior to the AS-truncation points. As far as static responsiveness is concerned, assume that the specifications call for $\frac{1}{1+KC_0P_0} < 0.05$. This implies that $K > 7.2$. Therefore, to achieve both good dynamic tracking and static responsiveness, K must satisfy

$$7.2 < K < 39. \qquad (18)$$

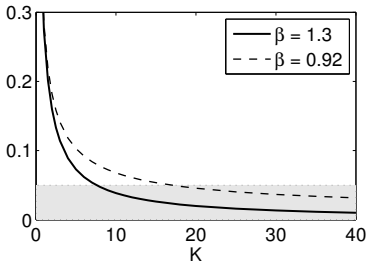

Fig. 10. The TE locus for Example 1 with $\beta = 0.92$ and $\beta = 1.3$.

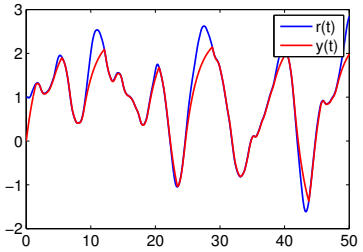

(a) $\beta = 0.92$.

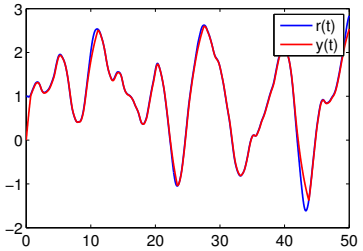

(b) $\beta = 1.3$.

Fig. 11. Responses of the system of Example 1.

B. Design for required steady state performance

Assume that the steady state specifications call for $|\mu_{\hat{e}}(K)| < \overline{\mu}_e$. Based on this specification, an admissible domain for TE can be introduced (see the shaded area in Fig. 10). For design, gain K must be selected such that the TE locus is in the admissible domain.

Returning to Example 1, assume that the specifications call for $|\mu_{\hat{e}}(K)| < 0.05$. The TE locus of the system, along with the admissible domain, is plotted in Fig. 10. As it follows from Fig. 10, the TE loci for $\beta = 0.92$ and $\beta = 1.3$ are in the admissible domain for $K > 17$ and $K > 7.6$, respectively.

Combining the above results, we conclude that, for the case of $\beta = 1.3$, for good static and dynamic tracking, K must satisfy

$$7.6 < K < 39.$$

Selecting $K = 35$, we illustrate the quality of tracking for both $\beta = 0.92$ and $\beta = 1.3$ in Fig. 11. Clearly, the quality of tracking is good for $\beta = 1.3$, but poor for $\beta = 0.92$ because of amplitude truncation.

There may be cases where the AS-poles and TE cannot be placed in their respective admissible domains simultaneously. An example of this situation is as follows.

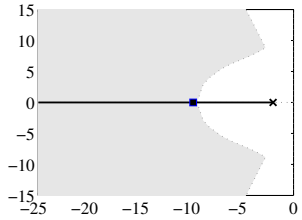

(a) AS-root locus.

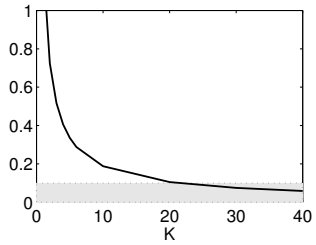

(b) TE locus.

Fig. 12. AS-root locus and TE locus of Example 2.

Example 2. Consider the system of Fig. 3(a) with

$$C(s) = 1, P(s) = \frac{3}{0.5s + 1}, \sigma_r = 1, \mu_r = 5, \alpha = 0, \beta = 2,$$

and $F_{\Omega_r}(s)$ as the third order butterworth filter (2) with bandwidth $\Omega_r = 2$. Assume that the steady state specifications call for $TE < 0.1$. The AS-root locus and TE locus of this system are plotted in Fig. 12. As it follows from the AS-root locus, to place the AS-poles within the admissible domain and prior to the truncation points, K must satisfy $1.24 < K < 1.33$. However, to place the TE within the admissible domain, K must satisfy $K > 21.5$. Clearly, no K satisfies both requirements. Fig. 13 shows the response of the system with $K = 1.3$ and $K = 22$. Clearly, with $K = 1.3$, dynamic tracking is good but there exist significant error in tracking of average values. With $K = 22$, the steady state tracking is good but significant output truncation occurs.

VI. Design of Step Tracking Controllers for Systems with Saturating Actuators

This section presents a method for designing controllers to track step reference signals in systems with saturating actuators. This method is based on the technique developed in Section V, and involves "converting" the dynamic part of the step tracking specifications to random signal tracking specifications. For the case of symmetric saturation, this method has been developed in [24]; here, we consider the general case.

Consider the system of Fig. 14, where all blocks are as before and $\mathbf{1}(t)$ denotes the unit step signal. Assume that the dynamic part of step tracking specifications are given by

$$\begin{aligned} &\text{Overshoot} \leq OS^*\%; \\ &\text{Settling time} \leq t_s^* \text{ sec}; \\ &\text{Rise time} \leq t_r^* \text{ sec}. \end{aligned} \tag{19}$$

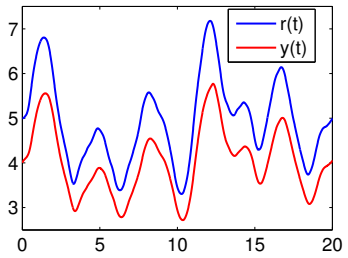

(a) $K = 1.3$.

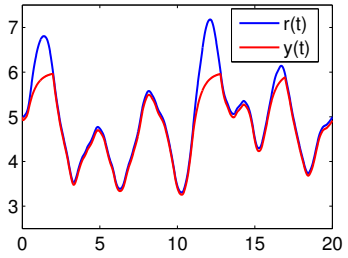

(b) $K = 22$.

Fig. 13. Response of the system of Example 2.

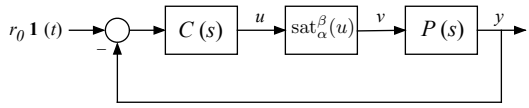

Fig. 14. LPNI system for tracking step signals.

To design step tracking controllers, we modify the block diagram of Fig. 14 to the one shown in Fig. 15. Here, the reference signal $r(t)$ is generated by filtering the step signal by a nominal second order system,

$$F_d(s) = \frac{\omega_n^2}{s^2 + 2\zeta\omega_n s + \omega_n^2}, \tag{20}$$

where ζ and ω_n are selected so that the output of $F_d(s)$ (i.e., $r(t)$) satisfies the dynamic specifications (19). If the specifications call for zero overshoot, ζ is selected to be one; otherwise, $0 < \zeta < 1$. The goal is to design a controller $C(s)$, if possible, such that the output $y(t)$ tracks well $r(t)$ and, therefore, satisfies the specs. To this end, we propose a method that consists of the following steps:

1) Convert the dynamic part of the step tracking specifications to random-signal tracking specifications. This is carried out by determining Ω_r from the specs (19) such that if a controller for the system of Fig. 3(a) tracks well the random reference $r(t)$ with this bandwidth, standard deviation $\sigma_r = r_0$, and mean $\mu_r = 0$, the same controller tracks well $r(t)$ in Fig. 15; we refer to this Ω_r as the *adjoint bandwidth* and denote it by Ω_a. An expression for calculating Ω_a is provided below.
2) Design such a controller for the system of Fig. 3(a) with $\Omega_r = \Omega_a$, using the method developed in Section V.
3) Finally, use the same controller in the system of Fig. 15. By doing so, we view the output of $F_d(s)$, i.e., $r(t)$, as the function to be tracked, rather than the step signal itself. In other words, $F_d(s)$ can be viewed as a pre-compensator in a 2 degree-of-freedom architecture [25].

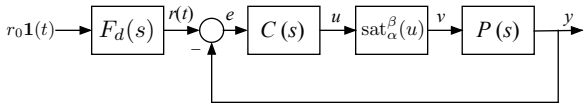

Fig. 15. The modified system for tracking steps.

The following proposition presents a formula for calculating the adjoint bandwidth.

Proposition 1. *Let $F_d(s)$ be the nominal second order transfer function* (20)*, whose step response satisfies specs* (19)*. If the specifications call for non-zero overshoot, then $0 < \zeta < 1$ and the adjoint bandwidth is given by*

$$\Omega_a = \sqrt{2}\omega_n \exp\left(-\frac{\sigma}{\omega_d}\tan^{-1}(\frac{\omega_d}{\sigma})\right), \tag{21}$$

where $\sigma = \zeta\omega_n$ and $\omega_d = \omega_n\sqrt{1-\zeta^2}$. If the specifications call for zero overshoot, a filter with $\zeta = 1$ is chosen, and the adjoint bandwidth is given by

$$\Omega_a = \sqrt{2}\omega_n e^{-1}. \tag{22}$$

The justification for the above proposition is given in [24], where it is shown that the adjoint bandwidth is defined by equating the maximum rate of change of $r(t)$ in Fig. 15 with the standard deviation of the rate of change of $r(t)$ in Fig. 3(a).

Example 3. Consider the system of Fig. 15 with

$$P(s) = \frac{150}{s^2 + 28s + 232}, \alpha = -3.5, \beta = 4.5.$$

The goal is to design a pre-compensator and controller such that the system tracks the unit step with the following specifications:

$$\begin{aligned} &\text{Steady state error} = 0; \\ &\text{Overshoot} \le 5\%; \\ &\text{Settling time} \le 1\,\text{sec}. \end{aligned} \tag{23}$$

Note that to meet the steady state specs, the controller must have a pole at the origin. As far as dynamic tracking is concerned, the pre-compensator is chosen as

$$F_d(s) = \frac{34}{s^2 + 8s + 34}, \tag{24}$$

from which the adjoint bandwidth is calculated to be $\Omega_a = 3.8$. Select a PI controller as follows:

$$C(s) = K\left(3 + \frac{75}{s}\right).$$

The AS-root locus is shown in Fig. 16, which enters the admissible domain. With $K = 1$, the AS-poles are within the admissible domain. The TE locus for this example is identically zero, so the steady state spec is met. For $K = 1$, the quality of tracking for the system of Figs. 3(a) and 15 are shown in Figs. 17(a) and 17(b), respectively. As can be

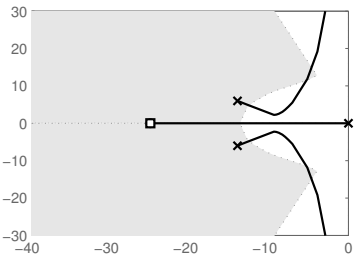

Fig. 16. S-root locus of Example 2.

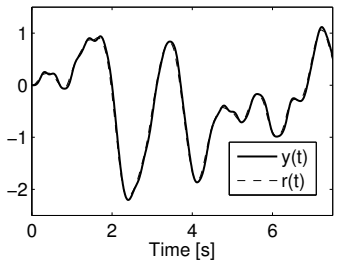

(a) Random reference tracking.

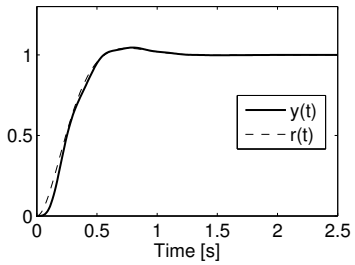

(b) Step tracking.

Fig. 17. Trajectories of the system in Example 2.

seen, the quality of tracking is good in both cases, and the step tracking specs are satisfied.

VII. Conclusions and Future Work

This paper shows that, unlike the S-LPNI case, A-LPNI systems are characterized by two performance loci: the usual – root locus (modified accordingly to account for saturation), and an additional one – tracking error locus (to account for non-classical behavior of steady state errors). In the design of reference tracking controllers, both must be taken into account, i.e., the gain of the controller should be selected so that both loci are in their respective admissible domains.

A number of topics related to this problem remain open. These include:

- Development of the performance loci approach to A-LPNI systems with saturation in both actuators and sensors.
- Development of the performance loci approach to A-LPNI systems with nonlinearities other than saturation.
- Design of disturbance rejection controllers for A-LPNI systems.
- Extension of LQR/LQG methods to A-LPNI systems.
- Extension of performance recovery techniques to A-LPNI systems.

Solution of these problems will result in a relatively complete QLC theory for A-LPNI systems.

Appendix

Proof of Theorem 1. Denote by K_e^* and $\mu_{\hat{u}}^*$ the limiting K_e and $\mu_{\hat{u}}$, i.e., $K_e^* = \lim_{K\to\infty} K_e(K), \mu_{\hat{u}}^* = \lim_{K\to\infty} \mu_{\hat{u}}(K)$. Define

$$\phi(K) = \left\| \frac{F_\Omega(s)C(s)}{1 + K_e(K)P(s)C(s)} \right\|_2 \sigma_r,$$

and let $\phi^* = \lim_{K\to\infty} \phi(K)$.

Then, applying Taylor series expansions to (8), we obtain

$$\begin{aligned} K_e(K) &= \frac{K}{2}\left[\text{erf}\left(\frac{\beta - \mu_{\hat{u}}(K)}{\sqrt{2}K\phi(K)}\right) - \text{erf}\left(\frac{\alpha - \mu_{\hat{u}}(K)}{\sqrt{2}K\phi(K)}\right)\right] \\ &= \frac{1}{\sqrt{\pi}}\left[\left(\frac{\beta - \mu_{\hat{u}}(K)}{\sqrt{2}\phi(K)}\right) - \frac{K}{3}\left(\frac{\beta - \mu_{\hat{u}}(K)}{\sqrt{2}K\phi(K)}\right)^3 + \cdots \right. \\ &\quad \left. - \left(\left(\frac{\alpha - \mu_{\hat{u}}(K)}{\sqrt{2}\phi(K)}\right) - \frac{K}{3}\left(\frac{\alpha - \mu_{\hat{u}}(K)}{\sqrt{2}K\phi(K)}\right)^3 + \cdots\right)\right]. \end{aligned} \tag{25}$$

We now consider four cases: (i) $K_e^* < \infty$, $\mu_{\hat{u}}^* = \infty$, (ii) $K_e^* = \infty$, $\mu_{\hat{u}}^* = \infty$, (iii) $K_e^* < \infty$, $\mu_{\hat{u}}^* < \infty$, (iv) $K_e^* = \infty$, $\mu_{\hat{u}}^* < \infty$.

Case (i) $K_e^* < \infty$, $\mu_{\hat{u}} = \infty$: Taking the limit of (25) as K tends to infinity, we obtain:

$$K_e^* = \lim_{K\to\infty} \frac{1}{\sqrt{\pi}} \frac{\beta - \alpha}{\sqrt{2}\phi^*}\left(1 - \frac{1}{3}\frac{3\mu_{\hat{u}}^2}{(\sqrt{2}K\phi^*)^2} + \frac{1}{10}\frac{5\mu_{\hat{u}}^4}{(\sqrt{2}K\phi^*)^4} - \cdots\right).$$

Define $\eta^* = \lim_{K\to\infty} \frac{\mu_{\hat{u}}(K)}{K\phi(K)}$. Then,

$$K_e^* = \frac{1}{\sqrt{\pi}} \frac{\beta - \alpha}{\sqrt{2}\phi^*} \sum_{n=0}^{\infty} \frac{1}{n!}(-(\frac{\eta^*}{\sqrt{2}})^2)^n = \frac{\beta - \alpha}{\sqrt{2\pi}\phi^*} e^{-\eta^{*2}/2}. \tag{26}$$

Using a similar approach, we expand the quasilinear bias equation (9) in Taylor series term by term:

- $\mu_{\hat{u}}(K)N_a(K) \to \frac{\beta-\alpha}{\sqrt{2\pi}}\eta^* e^{-\eta^{*2}/2}$.
- $-\frac{\beta}{2}\text{erf}(\frac{\beta-\mu_{\hat{u}}}{\sqrt{2}K\phi}) + \frac{\alpha}{2}\text{erf}(\frac{\alpha-\mu_{\hat{u}}}{\sqrt{2}K\phi}) \to \frac{\beta-\alpha}{2}\text{erf}(\eta^*/\sqrt{2})$.
- $\frac{K\phi}{\sqrt{2\pi}}[e^{-(\frac{\beta-\mu_{\hat{u}}}{\sqrt{2}K\phi})^2} - e^{-(\frac{\alpha-\mu_{\hat{u}}}{\sqrt{2}K\phi})^2}] \to \frac{\beta-\alpha}{\sqrt{2\pi}}\eta^* e^{-\eta^{*2}/2}$.

Therefore, by noting that

$$\lim_{K\to\infty} \mu_{\hat{u}}(K)/K = \eta^*\phi^*, \tag{27}$$

the bias equation becomes

$$\frac{\mu_r}{P_0} - \frac{\phi^*\eta^*}{C_0 P_0} = \frac{\alpha + \beta}{2} + \frac{\beta - \alpha}{2}\text{erf}(\eta^*/2).$$

This shows equations (12) and (13). Moreover, K_e^* is as in (26).

Case (ii) $K_e^* = \infty$, $\mu_{\hat{u}} = \infty$: Since $K_e^* = \infty$, (26) implies that $\phi^* = 0$ and the quasilinear bias equation implies that η^* is a finite number: $\eta^* = \sqrt{2}\text{erf}^{-1}(\frac{\frac{\mu_r}{P_0} - \frac{\alpha+\beta}{2}}{\frac{\beta-\alpha}{2}})$. Therefore, equations (12), (13) cover this case also. The proof of cases (iii) and (iv) is similar. ■

Proof of Theorem 2:

(Part a:) As $K \to 0$, $\hat{u} \to 0$ and $\hat{y} \to 0$. Therefore, $\mu_{\hat{e}} \to \mu_r$.

(Part b:) Rewrite equations (8) and (9) in the form of $F_1(K) = 0$ and $F_2(K) = 0$. Moreover, let $K_e(K)$ and $\mu_{\hat{u}}(K)$ be solutions to (8) and (9) for a given K. Using the implicit function theorem, it can be shown that

$$\frac{\partial \mu_{\hat{u}}(K)}{\partial K} = - \begin{vmatrix} \frac{\partial F_1}{\partial K} & \frac{\partial F_1}{\partial \mu_{\hat{u}}} \\ \frac{\partial F_2}{\partial K} & \frac{\partial F_2}{\partial \mu_{\hat{u}}} \end{vmatrix} \Big/ \begin{vmatrix} \frac{\partial F_1}{\partial K_e} & \frac{\partial F_1}{\partial \mu_{\hat{u}}} \\ \frac{\partial F_2}{\partial K_e} & \frac{\partial F_2}{\partial \mu_{\hat{u}}} \end{vmatrix}.$$

Then, computing each partial derivative and using Taylor series expansions to simplify them, it can be shown that as $K \to 0$, $\frac{\partial \mu_{\hat{u}}(K)}{\partial K} \to -KC_0\mu_r$. Therefore, using part (a), the result follows.

(Part c:) This part follows from (27).

(Part d:) This part follows from Definition 1. ■

REFERENCES

[1] S. Ching, Y. Eun, C. Gokcek, P. T. Kabamba, and S. M. Meerkov, *Quasilinear Control*. Cambridge University Press, 2010.

[2] I. Kazakov, "Approximate method for the statistical analysis of nonlinear systems," Technical Report VVIA 394, Trudy, 1954.

[3] R. Boonton, "Nonlinear control systems with random inputs," *IRE Trans. on Circuit Theory*, vol. 1, pp. 9–18, 1954.

[4] J. B. Roberts and P. D. Spanos, *Random Vibration and Statistical Linearization*. Dover Publications, 2003.

[5] I. Kazakov and B. Dostupov, *Statistical Dynamics of Nonlinear Control Systems*. Fizmatgiz, 1962, in Russian.

[6] A. Gelb and W. Vander Velde, *Multiple input describing function and nonlinear design*. New York: McGraw-Hill, 1968.

[7] H. K. Khalil, *Nonlinear Systems*, 3rd ed. Prentice Hall, 2002.

[8] M. A. Aizerman and F. R. Gantmacher, *Absolute Stability of Regulator Systems*. Holden-Day, 1964.

[9] C. Pittet, S. Tarbouriech, and C. Burgat, "Stability regions for linear systems with saturating controls via circle and Popov criteria," *Proceedings of the 36th IEEE Conference on Decision and Control*, pp. 4518–4523, 1997.

[10] A. Teel, "Semi-global stabilization of linear controllable systems with input nonlinearities," *IEEE Trans. Automat. Contr.*, vol. 40, pp. 96–100, 1995.

[11] A. Saberi, Z. Lin, and A. Teel, "Control of linear systems with saturating actuators," *IEEE Transactions on Automatic Control*, vol. 41, 1996.

[12] H. Hindi and S. Boyd, "Analysis of linear systems with saturation using convex optimization," *Proceedings of the 37th IEEE Conference on Decision and Control*, pp. 903–908, 1998.

[13] V. Kapila, A. Sparks, and H. Pan, "Control of systems with actuator saturation nonlinearities: an lmi approach," *International Journal of Control*, vol. 74, pp. 586–599, 2001.

[14] A. Saberi, A. Stoorvogel, and P. Sannuti, *Internal and External Stabilization of Linear Systems with Constraints*. Birkhauser, 2012.

[15] E. G. Gilbert and I. Kolmanovsky, "Discrete-time reference governors and the nonlinear control of systems with state and control constraints," *International Journal of robust and nonlinear control*, vol. 5, 1995.

[16] A. Bemporad and M. Morari, "Control of systems integrating logic, dynamics, and constraints," *Automatica*, vol. 35, 1999.

[17] E. F. Camacho and C. B. Alba, *Model Predictive Control*. Prentice Hall, 2000.

[18] M. Morari, C. Garcia, D. Prett, and J. Lee, *Model Predictive Control*. Prentice Hall – PTR, 2004.

[19] M. V. Kothare, P. J. Campo, M. Morari, and C. N. Nett, "A unified framework for the study of anti-windup designs," *Automatica*, vol. 30, no. 12, pp. 1869–1883, 1994.

[20] A. Zheng, M. V. Kothare, and M. Morari, "Anti-windup design for internal model control," *Int. J. Contr.*, vol. 60, pp. 1015–1024, 1994.

[21] N. Kapoor, A. Teel, and P. Daoutidis, "An anti-windup design for linear systems with input saturation," *Automatica*, vol. 34, no. 5, pp. 559–574, 1998.

[22] L. Zaccarian and A. Teel, *Modern Anti-windup Synthesis: Control Augmentation for Actuator Saturation*. Princeton University Press, 2011.

[23] P. Kabamba, S. Meerkov, and H. R. Ossareh, "Performance analysis of feedback systems with asymmetric nonlinear actuators and sensors," submitted for publications to the International Journal of Robust and Nonlinear Control. [Online]. Available: www-_personal.umich.edu/~hamido/papers/QLC/asymmetric.pdf

[24] ——, "A method for designing step-tracking controllers for systems with saturating actuators," accepted for presentation at the *2013 American Control Conference* in Washington DC.

[25] G. C. Goodwin, S. F. Graebe, and M. E. Salgado, *Control System Design*. Prentice Hall, 2000.